01,05

Simulation of two-vortex spin-transfer nano-oscilators with maximum operating frequency

© E.G. Ekomasov[1], D.F. Neradovsky[2], G.I. Antonov[1], V.V. Filippova[3]

[1] Ufa University of Science and Technology,
Ufa, Russia
[2] University of Tyumen,
Tyumen, Russia
[3] Institute of Molecule and Crystal Physics, Subdivision of the Ufa Federal Research Centre
of the Russian Academy of Sciences,
Ufa, Russia

E-mail: georgij.antonow@yandex.ru

Received December 24, 2023
Revised February 5, 2024
Accepted February 5, 2024

The influence of spin-polarized current and the thickness of magnetic layers on the coupled dynamics of vortices in small-diameter spin-transfer nanooscillators is studied. The nanooscillator has two magnetic permalloy layers (containing magnetic vortices), separated by a non-magnetic copper layer. Using analytical and numerical methods, the nonlinear dynamics of two magnetostatically coupled magnetic vortices under the influence of a spin-polarized electric current was studied. Numerical calculations of the dynamics of magnetostatically coupled vortices were carried out using the SpinPM micromagnetic modeling software package. Conditions have been found for obtaining a maximum frequency in such systems and increasing the range of currents in which a stationary mode of coupled vortex oscillations is observed. For the case of two identical magnetic layers, the possibility of the emergence of new scenarios of coupled vortex dynamics is shown.

Keywords: magnetic vortex, spin-transfer nanooscillator, nanocylinders.

DOI: 10.61011/PSS.2024.03.57932.274

1. Introduction

Spin-transfer nanooscillators (STNOs) are often designed as three-layer magnetic nanocylinders [1–3]. Vortex STNOs are characterized by the presence of a magnetic vortex in their magnetic layer (or in both magnetic layers). The dynamics of this vortex enables microwave emission. Note that the practical interest in such structures is not limited to STNO microwave generators. Vortex multibit random-access memory, where data is stored in the form of topological states of a vortex, has also been designed [4,5]. In addition, vortex spintronic structures and their ensembles are being examined in the context of neuromorphic devices implementing reservoir computing [6].

A magnetic vortex may be a ground state in permalloy nanodisks of a certain size [7,8]. In qualitative terms, the magnetic structure of a vortex at the center of a disk in equilibrium conditions is as follows: the magnetization field is in-plane and winds about the vortex center. In a small neighborhood of the disk center, the magnetization goes out of plane and is oriented perpendicularly to it. This central part is called the vortex core and has a diameter on the order of 10 nm. The micromagnetic structure of a vortex and its core has been observed experimentally numerous times [9–10]. The dynamics of magnetic vortices confined in micrometer-sized permalloy disks 30 nm in thickness has also been visualized directly via X-ray photoemission spectroscopy [11].

The dynamics of a vortex in a single-vortex STNO has been studied in detail. It has been demonstrated that spin-polarized current allows one to control the dynamics and the structure of vortices [12–13]). Spin-polarized current may induce magnetization oscillations. The gyrotropic mode corresponds to circular translational motion of a vortex in a disc around its center. It has been demonstrated that Thiele's equations may be used to characterize gyrotropic vortex motion. A method for derivation of equations based on the collective variables technique for gyroscopic vortex dynamics in a nanodisk was presented, e.g., in [14–16]. An analytical ansatz proposed in [17], which characterizes the structure of a static magnetic vortex minimizing the magnetostatic energy, was used to derive these equations. It was found that the frequency of oscillations of the vortex core about the geometric center of a nanodisk depends linearly on the ratio of geometric dimensions of this disk. A theoretical description of the dynamics of vortices under the influence of spin current was obtained, and the dependence of frequency of a single-vortex STNO on the spin-polarized current density was characterized.

The dynamics of magnetostatically coupled magnetic vortices in two-vortex STNOs is less well understood (see, e.g., [1,18–25]). The properties of this system depend largely on the mutual orientation of magnetization in vortex

cores. The number of possible states, which are characterized by the polarity and chirality parameters of vortices, suitable for practical applications (e. g., magnetic memory) increases in such a system of coupled vortices. The authors of experimental studies [19–23] have successfully used spin-polarized current and a magnetic field to perform independent selection and control of the needed vortex chiralities and polarities in a trilayer STNO containing vortices in each of its two magnetic layers. Coupled vortex dynamics provides an opportunity to reduce the spectrum width considerably even in zero field and, consequently, has strong potential for application as a means to enhance the quality of spintronic microwave signal generators. Effective Thiele's equations were used to characterize the dynamics of coupled vortices in [18], and the gyrotropic frequency of stationary coupled oscillations was found. Stationary vortex dynamics has two solutions in this case. One of them lies above the frequency determined for a single vortex, and the other is below it. Note that the obtained solutions agree qualitatively with the available experimental data. The results of numerical modeling of the dynamics of coupled vortices in [26–30] for a circular vortex STNO with permalloy magnetic layers, which has earlier been studied experimentally, provided insight into those features of coupled vortex dynamics that could not be examined in experiments. Different thicknesses of thick (15 nm) and thin (4 nm) magnetic layers and different diameters of nanodisks (120, 200, and 400 nm) with vortices having the same initial chiralities and polarities were considered. In the present study, the influence of thickness of magnetic layers on the stationary dynamics of vortices is analyzed with the aim of determining the structure of a trilayer STNO that has the maximum possible frequency of stationary vortex oscillations.

2. Main equations and results of analytical calculations

Let us examine a trilayer nanocylinder containing two magnetic permalloy layers with thickness L_1 and L_2 and a non-magnetic interlayer with thickness d (Figure 1).

The permalloy (denoted as Py) composition is $Ni_{80}Fe_{20}$. It is assumed that a magnetic vortex exists as a ground state in each magnetic layer. Effective equations for vectors $\mathbf{r}_1(t)$ and $\mathbf{r}_2(t)$, which specify the positions of centers of vortices, may be used for a rough analytical examination of the stationary dynamics of such vortices [18]:

$$\mathbf{G}_i \times \mathbf{r}_i - \frac{\partial W(\mathbf{r}_1, \mathbf{r}_2)}{\partial \mathbf{r}_i} = 0, \qquad (1)$$

where $\mathbf{G}_i = -G_i \mathbf{e}_z$, $G_i = 2\pi L_i \frac{M_{iS}}{\gamma}$, M_{iS} is the saturation magnetization of the ith vortex, γ is the gyromagnetic ratio, L_i is the thickness of the ith magnetic layer, and $W(\mathbf{r}_1, \mathbf{r}_2)$ is the potential energy of a system of two coupled vortices that

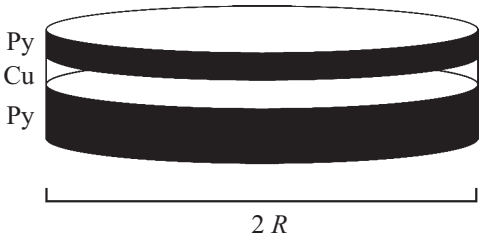

Figure 1. Schematic diagram of a three-layer nanocolumnar structure.

has the form

$$W(\mathbf{r}_1, \mathbf{r}_2) = \frac{1}{2} k_1 \mathbf{r}_1^2 + \frac{1}{2} k_2 \mathbf{r}_2^2 + \mu \mathbf{r}_1 \mathbf{r}_2, \qquad (2)$$

where K_i is the coefficient of quasi-elasticity of the ith vortex and μ is the coefficient characterizing the magnetostatic coupling of vortices. Let us assume that the solutions of Eqs. (1) in the steady-state mode have the form of harmonic oscillations

$$\mathbf{r}_j(t) = \mathbf{r}_{0j} \cdot \exp(i\omega t), \quad j = 1, 2. \qquad (3)$$

With (2) and (3) taken into account, the following system of equations is derived from (1):

$$G\omega \mathbf{r}_1 - k_1 \mathbf{r}_1 - \mu \mathbf{r}_2 = 0,$$

$$\gamma p G \omega \mathbf{r}_2 - k_2 \mathbf{r}_2 - \mu \mathbf{r}_1 = 0, \qquad (4)$$

where $G_1 = G$, $G_2 = \gamma p G$.

Roots of the characteristic equation of system (4) take the form

$$\omega_{1,2} = \frac{k_1}{G_1}\left(1 - \frac{1}{2}\left(1 - \frac{k_2}{k_1 \gamma p}\right) \mp \frac{1}{2}\sqrt{\left(1 - \frac{k_2}{k_1 \gamma p}\right)^2 + \frac{4\mu^2}{\gamma p k_1^2}}\right). \qquad (5)$$

The expressions for eigen frequencies of oscillations of a system of two coupled vortices may be written as

$$\frac{\omega_{1,2}}{\omega_{01}} = 1 + \beta_{1,2}(\chi), \qquad (6)$$

where

$$\beta_{1,2}(\chi) = \frac{1}{2}\left[-\left(1 - \frac{k_{21}}{G_{21}}\right) \mp \sqrt{\left(1 - \frac{k_{21}}{G_{21}}\right)^2 + \frac{4\chi^2}{G_{21}}}\right]. \qquad (7)$$

Index „1" in formula (7) corresponds to the minus sign before the root, while index „2" corresponds to the plus sign.

Let us analyze the obtained solutions with a view to answering the question of which of the possible types of a trilayer nanocylinder has the maximum vortex oscillation

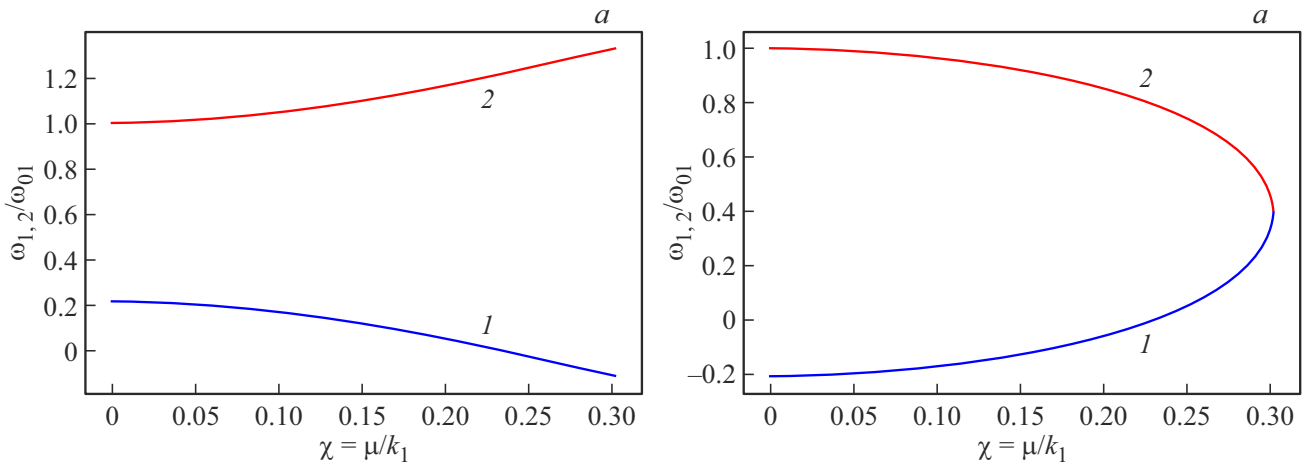

Figure 2. Dependences of normalized frequencies $\omega_{1,2}/\omega_{01}$ on dimensionless parameter χ. *a* — The case of identical vortex polarities; *b* — the case of different polarities.

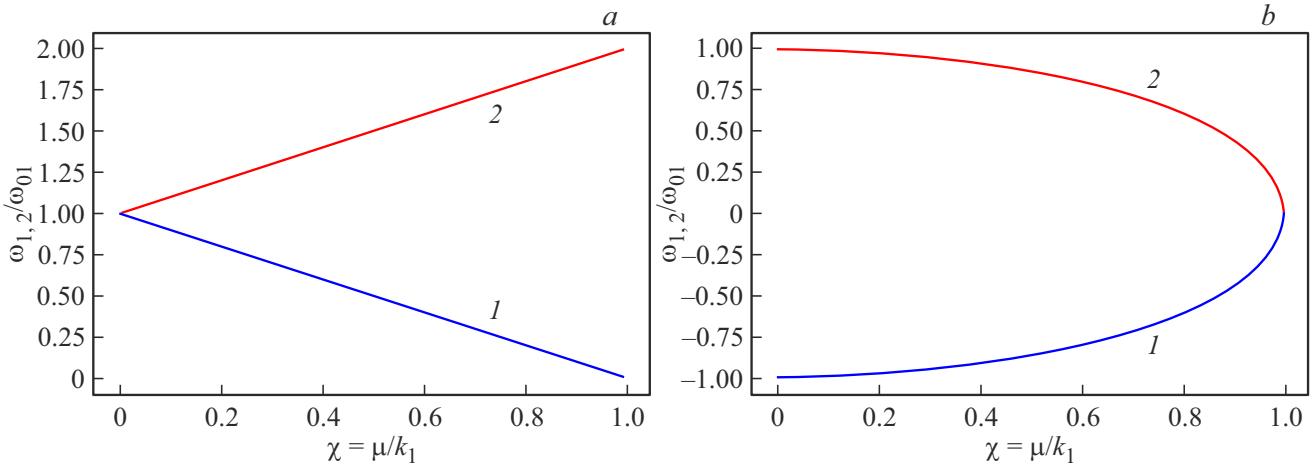

Figure 3. Dependences of normalized frequencies $\omega_{1,2}/\omega_{01}$ on dimensionless parameter χ for two identical layers. *a* — The case of identical vortex polarities; *b* — the case of different polarities.

frequency. In the case of vortices of parallel polarities, $p = +1$, $G_{21} > 0$, and the radical expression in (7) is positive. This implies that in the linear approximation, eigen frequencies of oscillations of a system of coupled vortices with the same polarity exist at an arbitrary value of parameter μ/k_1. In the case of vortices of antiparallel polarities, $p = -|p| = -1$. Let us determine the values of $\mu/k_1 = \chi$ at which the radical expression becomes zero. With the $p = -|p|$ sign choice taken into account, we write the equation

$$-\frac{4\chi^2}{\gamma|p|} + \left(1 + \frac{k_{21}}{\gamma|p|}\right)^2 = 0. \tag{8}$$

Since it is implied that $\mu/k_1 = \chi > 0$, a positive root is obtained:

$$\chi_k = \frac{1}{2}\sqrt{\gamma|p|}\left(1 + \frac{k_{21}}{\gamma|p|}\right).$$

Thus, eigen frequencies of oscillations of vortices with different polarities exist if

$$0 \le \chi \le \frac{1}{2}\sqrt{\gamma|p|}\left(1 + \frac{k_{21}}{\gamma|p|}\right). \tag{9}$$

The limit value of frequency in this case is

$$\omega_1 = \omega_2 = \omega_{01}\frac{1}{2}\left(1 - \frac{k_{21}}{\gamma|p|}\right). \tag{10}$$

The values of mentioned parameters for a trilayer structure with a 10-nm-thick non-magnetic layer and permalloy magnetic nanodisks 120 nm in diameter and 15 and 4 nm in thickness, which has been examined experimentally in [21], are $\gamma = 0.25$ and $k_2/k_1 = k_{21} = 1/19$. Figure 2 presents the dependences of normalized frequencies $\omega_{1,2}/\omega_{01}$ on χ for parallel and antiparallel vortex polarities in magnetic layers of various thickness. Figure 3 shows the result of the same

calculation for two identical layers with $k_2/k_1 = k_{21} = 1$, $G_2/G_1 = G_{21} = 1$. It can be seen that a significant enhancement of the frequency of stationary vortex oscillations may be achieved in the case of vortices of parallel polarities. Notably, the oscillation frequency corresponding to identical magnetic layers of a greater thickness is higher. The eigen frequency of stationary oscillations of a single vortex in a nanodisk is proportional to its thickness [7]. This is the reason why identical magnetic layers of a greater thickness provide a higher oscillation frequency.

Formulae for calculation of phenomenological parameters k, μ in the case of identical magnetic layers were proposed in [17]. Let us calculate these parameters for a magnetic disk 120 nm in diameter and 15 nm in thickness. The following dimensionless parameters are introduced for this purpose: $\beta = L/R$ and $d_s = d/R$, where R is the disk radius and d is the non-magnetic interlayer thickness. Magnetostatic interaction parameter μ is calculated as [17]

$$\mu = 8\pi^2 M_s^2 R F(\beta, d_s) C_1 C_2, \tag{11}$$

where C_1, C_2 are the parameters of chirality of the corresponding vortices.

It is assumed below that chirality $C_1 = C_2 = 1$. Note that the eigen frequencies of vortices in the above-discussed linear model are independent of chirality, since coefficient μ in the formula for frequency (see (5)) is raised to the second power. Function $F(\beta, d_s)$ in (10) is given by [17]

$$F(\beta, d_s) = \int_0^\infty t^{-2} e^{-d_s t} (1 - e^{-\beta t})^2 I^2(t) dt. \tag{12}$$

Function $I(t)$ is calculated via the first-order Bessel function as

$$I(t) = \int_0^1 x J_1(tx) dx, \tag{13}$$

The formula for quasi-elasticity coefficient k is [17]

$$k = 4\pi M_s^2 L \left(4\pi F_0(\beta) - 0.5 \left(\frac{R_0}{R} \right)^2 \right), \tag{14}$$

where

$$F_0(\beta) = \int_0^\infty t^{-1} \left(1 - \frac{1 - e^{-\beta t}}{\beta t} \right) I^2(t) dt,$$

$I(t)$ is calculated in accordance with Eq. (13), $R_0 = \sqrt{\frac{2A}{M_s^2}}$ is the „exchange“ length, and A is the exchange interaction constant. The sought-for μ/k ratio is derived from formulae (11) and (14):

$$\frac{\mu}{k} = \frac{2\pi}{\beta} \frac{F(\beta, d_s)}{4\pi F_0(\beta) - 0.5(R_0/R)^2}. \tag{15}$$

To obtain a numerical estimate of this ratio, we set magnetic layer thickness $L = 15$ nm, non-magnetic interlayer thickness $d = 10$ nm, and cylinder radius $R = 60$ nm. The saturation magnetization for permalloy is $M_s = 700\,\text{erg}/(\text{G} \cdot \text{cm}^3)$, and the exchange constant is $A = 1.2 \cdot 10^{-6}$ erg/cm. Having calculated the corresponding integrals In (15), we find $\mu/k \approx 0.656$.

3. Results of numerical calculations

Numerical calculations of the nonlinear magnetization dynamics were carried out based on the generalized Landau–Lifshitz equation (GLLE). It contains additional torque $T_{s.t.}$, which governs the interaction of spin-polarized current with magnetization, and has the form [12]

$$\dot{\mathbf{M}} = -[\mathbf{M} \times \mathbf{H}_{\text{eff}}] + \frac{\alpha}{M_s} [\mathbf{M} \times \dot{\mathbf{M}}] + T_{s.t.}, \tag{16}$$

where $\mathbf{M}$ is the magnetization vector, M_s is the saturation magnetization, γ is the gyromagnetic ratio, α is the Gilbert damping parameter, and effective field $\mathbf{H}_{\text{eff}}$ sums the contributions from the external magnetic field and the magnetostatic and exchange interaction fields. Following [12], we write the torque as

$$T_{s.t.} = \frac{\gamma a_j}{M_s} \times \mathbf{M}[\mathbf{M} \times \mathbf{m}_{\text{ref}}] + \gamma b_j \mathbf{M} \times \mathbf{m}_{\text{ref}}, \tag{17}$$

$$a_j = \frac{\hbar}{2|e|} \frac{1}{d} P \frac{1}{M_s} J_e, \quad b_j = \beta a_j, \quad \beta \approx 0.05 - 0.2.$$

Here, $\hbar$ is the Planck constant, e is the electron charge, d is the layer thickness, J_e is the current density, P is the current polarization, and $\mathbf{m}_{\text{ref}}$ is a unit vector directed along the reference layer magnetization.

Coupled vortex dynamics in trilayer nanocylinders 120 nm in diameter with permalloy magnetic layers differing in thickness (15 and 4 nm) has already been examined numerically and experimentally in [19,21,26,30]. However, the above analytical results demonstrate that the frequency of stationary oscillations of an STNO with magnetic nanodisks of the same thickness and diameter should be higher. Therefore, we examine two identical permalloy magnetic layers with a thickness of 15 nm. The motion of coupled magnetic vortices in nanocolumn is induced by spin-polarized current that is perpendicular to the disk surface plane. The magnetic parameters for a nanodisk 15 nm in thickness are as follows [21]: $M_s = 700\,\text{erg/G} \cdot \text{cm}^3$ and exchange stiffness $A = 1.2 \cdot 10^{-6}$ erg/cm. Gilbert damping parameter $\alpha = 0.01$, gyromagnetic ratio $\gamma = 2.0023 \cdot 10^7\,(\text{Oe} \cdot \text{s})^{-1}$, and current polarization $P = 0.1$. It was assumed that the current flowing through the cross section of a column is uniform. At the initial time, the chiralities of vortices were identical and corresponded to the direction of the current-induced Oersted field. The polarities of both vortices were directed upward.

It should be noted that the dynamics of magnetization of both magnetic layers was modeled; therefore, mref is spatially nonuniform, depends on time, and is determined

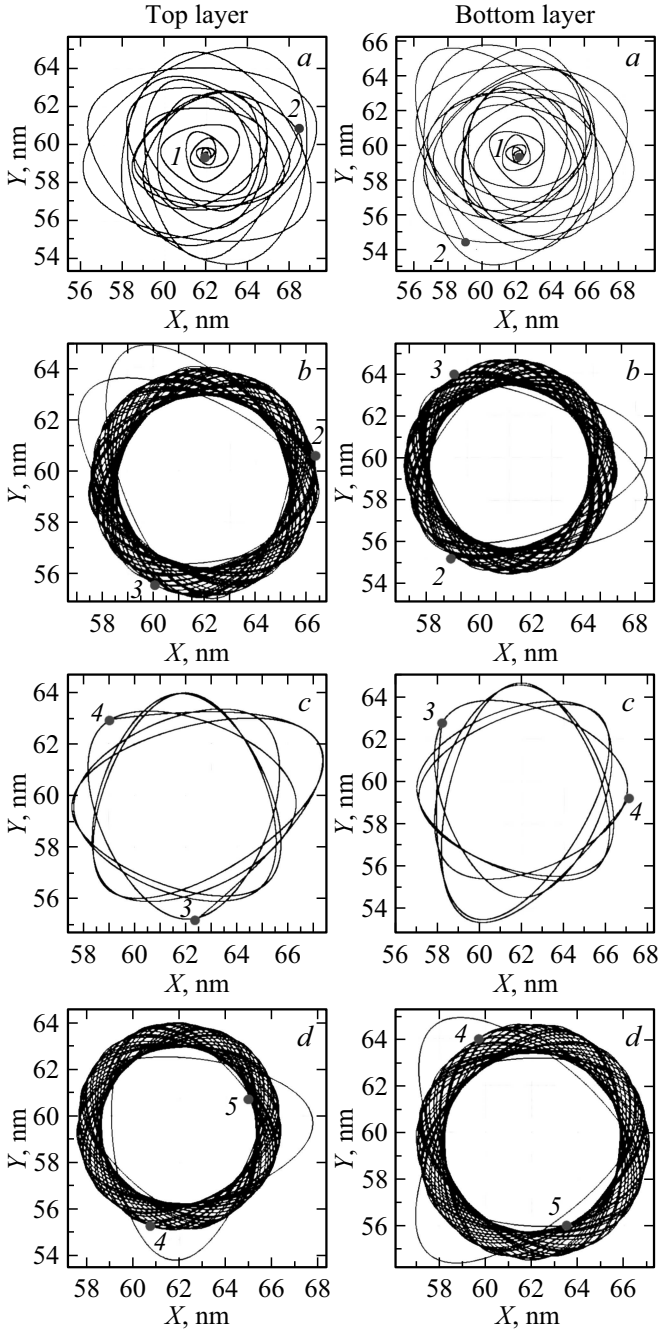

Figure 4. Trajectory of motion of the vortex center in the top (left panel) and bottom (right panel) magnetic layers in the 15/15 case: *a* — 0–10 ns, *b* — 25–50 ns, *c* — 42–45 ns, *d* — 80–100 ns.

by solving the GLLE numerically within the entire system. Micromagnetic modeling was performed via numerical integration of Eq. (1) with the use of the SpinPM code, which is based on the fourth-order Runge–Kutta method with time-step adaptation for integration over time. The dynamics of two vortices was examined on an equal basis (i.e., the bottom layer acts as a spin polarizer on the top one, and vice versa; both vortices are moving; and the full-scale magnetostatic interaction between layers is considered). This code and method have already been proven efficient in numerical modeling of the dynamics of coupled magnetic vortices (see, e.g., [21,28,31,32]).

The trajectory of the vortex center coordinate is assumed to be the vortex trajectory. The vortex center is a point where the magnetization component perpendicular to the nanocolumn plane reaches its maximum. Figure 4 presents the trajectories of vortex motion in the top and bottom magnetic layers at a current of 28.27 mA. The following time points are numbered: *a*) *1* — 0 ns, *2* — 10 ns; *b*) *2* — 25 ns, *3* — 50 ns; *c*) *3* — 42 ns, *4* — 45 ns; and *d*) *4* — 80 ns, *5* — 100 ns. It can be seen that these points start moving with a certain acceleration when current is switched on. At the onset of the stationary oscillation mode of the system of coupled vortices, the trajectory assumes the shape of a shifting smoothed triangle (see Figure 4). Both vortices move along a shifting elliptical orbit within the time interval from 42 to 45 ns. The lag of the second vortex with respect to the first one is not compensated and remains equal to 1/3 of a turn. The trajectory at 80–100 ns indicates that the vortex motion pattern remains virtually unchanged. Thus, the plotted shifting elliptical trajectory has the shape of a ring. In view of this, the problem of determination of the vortex oscillation frequency arises. Therefore, two methods for determining the effective oscillation frequency were used: the common technique of frequency calculation from the oscillation period derived from the plotted time dependence of mean x-component of magnetization $\langle M_x(t)\rangle$ and Fourier analysis. The comparison of obtained frequencies revealed that these two methods yield roughly the same results. The difference between them is within 0.01–0.03 GHz, which is on the order of 1–3% of the frequency value. The settling time of vortex dynamics is on the order of 40 ns and is almost independent of the current magnitude (see Figure 5). The dependence of the frequency of stationary coupled vortex oscillations on the magnitude of spin-polarized current is shown in Figure 6. The frequency depends almost linearly on current. Note that, in accordance with theoretical predictions, vortices move with a frequency significantly higher (almost 2 GHz) than the one obtained in the 15/4 case of magnetic disks of different thickness (the frequency here is just above 1.1 GHz). However, the critical current of transition to the stationary mode increases manyfold. The first critical current for an STNO with 15/4 magnetic layers was 4.64 mA [26]. The same current in the present study is 21.2 mA. The range of currents supporting stationary oscillations was also expanded.

Let us determine the frequency of coupled vortex oscillations at zero current, which is needed for comparison with the results of analytical calculations from the previous section. Extrapolating the curve in Figure 6 to its intersection with the vertical axis, we find a value of 1.805 GHz. The eigen frequency of an individual magnetic disk may be determined using the following formula [16]:

$$\omega_0 = \gamma 2.218 \frac{L}{R} M_s. \qquad (18)$$

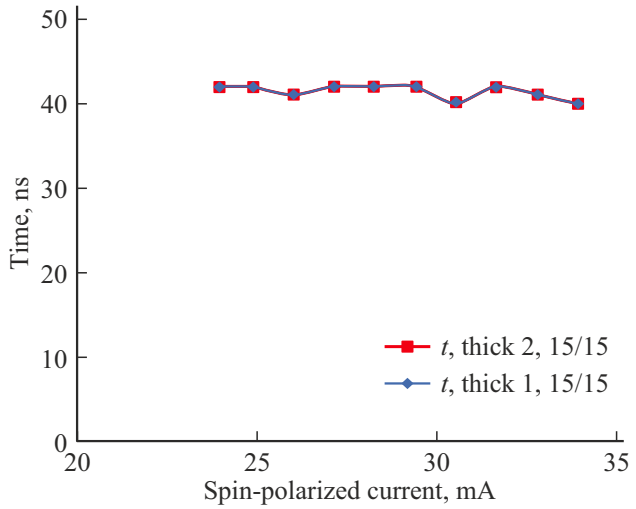

Figure 5. Dependence of the settling time of oscillations of coupled vortices on the current magnitude, the 15/15 case.

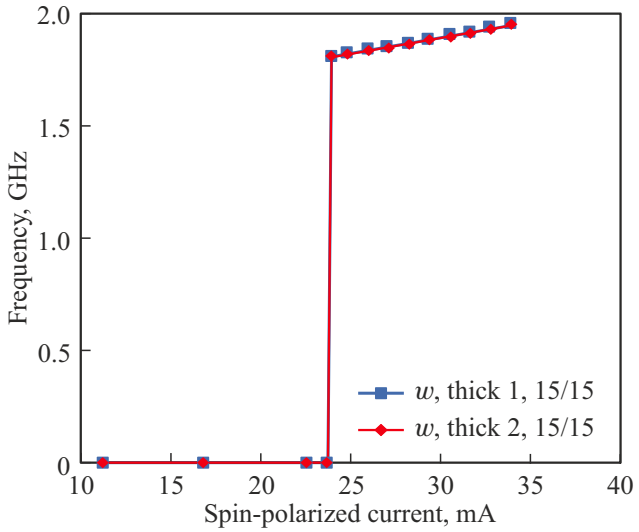

Figure 6. Dependence of the frequency of stationary coupled vortex oscillations on the magnitude of spin-polarized current in the 15/15 case.

In the present case, $\omega_0 \approx 1.23$ GHz. It then follows from (6) and (7) that $\chi_m = \frac{\omega}{\omega_0} - 1$. Inserting numerical values, one may determine dimensionless parameter $\chi_m \approx 0.476$ and compare it to the calculated $\chi_p \approx 0.656$ value obtained using formula (15). It follows from this comparison that the difference between the more accurate numerical value and the analytical value of parameter $\chi_m = \mu/k$ is on the order of 30%, which indicates that the above analytical model is applicable in qualitative analysis of the dynamics of coupled vortices.

To complete the picture, let us examine the case of identical magnetic layers with a thickness of 4 nm. The magnetic parameters for a 4-nm-thick nanodisk are as follows [21]: $M_s = 600$ erg/G $\cdot$ cm^3, $A = 1.12 \cdot 10^{-6}$ erg/cm, Gilbert damping parameter $\alpha = 0.01$, gyromagnetic ratio $\gamma = 2.0023 \cdot 10^7$ (Oe $\cdot$ s)$^{-1}$, and current polarization $P = 0.1$. Figure 7 presents the trajectories of vortex motion at a current of 6.67 mA. It can be seen that this trajectory of motion of the vortex center has certain features distinguishing it from the stationary-mode trajectory in the 15/4 case examined in [26]. As in the 15/15 case, the second vortex lags behind the first one. At the initial stage

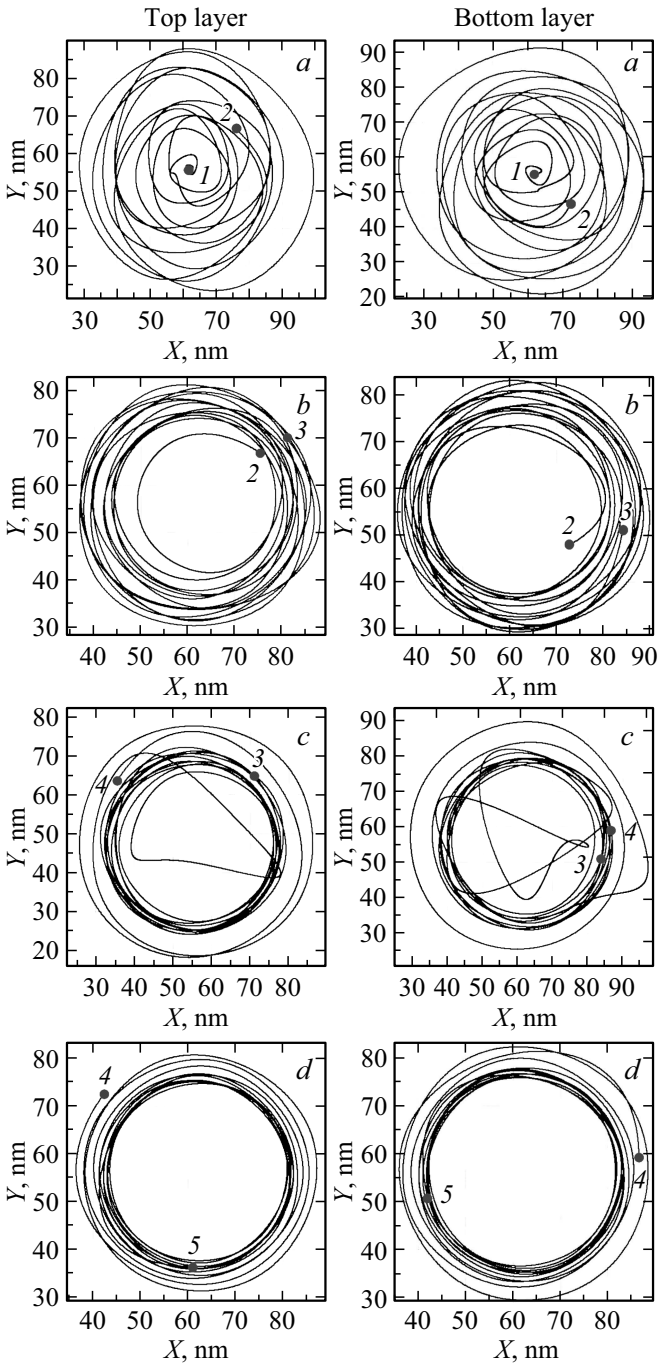

Figure 7. Trajectory of motion of the vortex center in the top (left panel) and bottom (right panel) layers in the 4/4 case at a current of 6.67 mA: *a* — 0–25 ns, *b* — 25–50 ns, *c* — 50–75 ns, *d* — 75–100 ns.

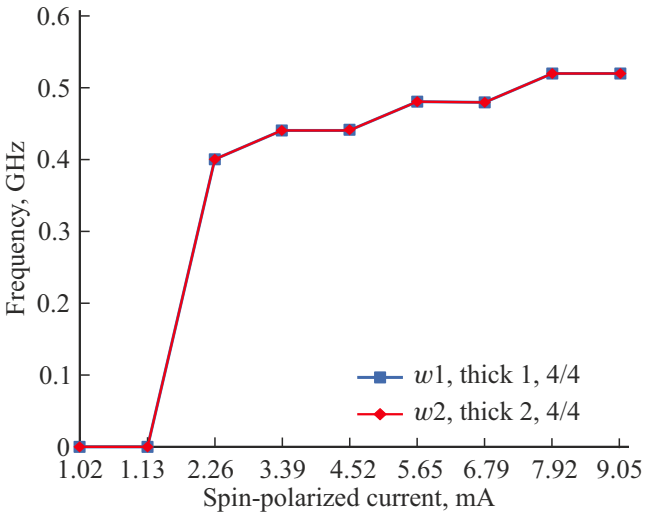

Figure 8. Dependence of the frequency of stationary oscillations on the magnitude of spin-polarized current in the 4/4 case.

of motion (0−25 ns, point 1−0 ns), vortices first spin in an expanding orbit, but their motion trend then shifts to spinning in a decaying orbit at a certain point in time. At the next stage (25−50 ns, point 2−25 ns), vortices again start spinning in an expanding orbit, but the magnitude of its expansion is smaller than the one observed before. A loop standing out from the common circle is seen within the 50−75 ns time range (point 3−50 ns). The decaying orbit trend emerges again within the 75−100 ns time range (point 4−75 ns). Thus, a new coupled vortex dynamics mode is seen: periodic transitions from stationary oscillations along a small radius to stationary oscillations along a large radius, and vice versa. The time period of this transition exceeds significantly the period of stationary oscillations of vortices about the center. Figure 8 presents the current dependence of the fundamental frequency of the stationary mode of vortex center oscillations. The eigen frequency for an individual magnetic disk is $\omega_0 \approx 0.32$ GHz. The first critical current starts from 2.26 mA, and the frequency is 0.4 GHz. These values are lower than the ones for an STNO with 15/4 magnetic layers. The frequency increases almost linearly with current.

4. Conclusion

The influence of spin-polarized current and the thickness of magnetic layers on coupled vortex dynamics in small-diameter spin-transfer nanooscillators was examined analytically and numerically. The parameters of a two-vortex trilayer STNO with the maximum oscillation frequency in the stationary mode were determined with the use of effective coupled dynamics equations for vortex centers. STNOs 120 nm in diameter with the sizes of Py(4)/Cu(10)/Py(4) and Py(15)/Cu(10)/Py(15) were studied numerically with the SPIN PM code. Vortex motion trajectories were characterized. In the 15/15 case, the stationary-mode trajectory changed significantly relative to a circular orbit that is typical of the 4/15 case examined earlier; a shift of the circular orbit became apparent. In the 4/4 case, a new type of trajectory with slow periodic transitions of a vortex from a lower circular motion orbit to a higher one was observed. Current dependences of the stationary vortex orbit frequency were plotted. The frequency depends linearly on current in both cases. As was predicted analytically, the maximum frequency rise is achieved in the 15/15 case. However, the magnitudes of critical currents also increase under these conditions.

Conflict of interest

The authors declare that they have no conflict of interest.

References

[1] K.A. Zvezdin, E.G. Ekomasov. Phys. Met. Metallografy **123**, *3*, 219 (2022).
[2] A. Hamadeh, N. Locatelli, V.V. Naletov, R. Lebrun, G. Loubens, J. Grollier, O. Klein, V. Cros. Phys. Rev. Lett. **112**, 257201 (2014).
[3] B. Dieny, I.L. Prejbeanu, K. Garello, P. Gambardella, P. Freitas, R. Lehndorff, W. Raberg, U. Ebels, S.O. Demokritov, J. Akerman, A. Deac, P. Pirro, C. Adelmann, A. Anane, A.V. Chumak, A. Hirohata, S. Mangin Sergio, O. Valenzuela, M. Cengiz Onbaşlı, M. d'Aquino, G. Prenat 1, G. Finocchio, L. Lopez-Diaz, R. Chantrell, O. Chubykalo-Fesenko, P. Bortolotti. Nature Electron. **3**, 446 (2020).
[4] S. Bohlens, B. Krüger, A. Drews, M. Bolte, M. Guido, D. Pfannkuche. Appl. Phys. Lett. **93**, *14*, *142*, 508(2008).
[5] K. Nakano, D. Chiba, N. Ohshima, S. Kasai, T. Sato, Y. Nakatani, K. Sekiguchi, K. Kobayashi, T. Ono. Appl. Phys. Lett. **99**, *262*, 505 (2011).
[6] J. Grollier, D. Querlioz, K.Y. Camsari, K. Everschor-Sitte, S. Fukami, M.D. Stiles. Nature Electron. **3**, 360 (2020).
[7] K.Y. Guslienko. J. Nanosci. Nanotechnology **8**, 2745 (2008).
[8] K.L. Metlov, Y. Pak Lee. Appl. Phys. Lett. **92**, *112*, 506(2008).
[9] M. Schneider, H. Hoffmann, J. Zweck. Appl. Phys. Lett. **77**, 2909 (2000).
[10] T. Shinjo, T. Okuno, R. Hassdorf, K. Shigeto, T. Ono. Science **289**, 930 (2000).
[11] K.Y. Guslienko, X.F. Han, D.J. Keavney, R. Divan, S.D. Bader. Phys. Rev. Lett. **96**, 197 (2017).
[12] A.K. Zvezdin, A.V. Khval'kovskii, K.A. Zvezdin. Phys.-Usp. **51**, *4*, 412 (2008).
[13] A. Dussaux, B. Georges, J. Grollier, V. Cros, A.V. Khvalkovskiy, A. Fukushima, M. Konoto, H. Kubota, K. Yakushiji, S. Yuasa, K.A. Zvezdin, K. Ando, A. Fert. Nature Commun. **1**, 8 (2010).
[14] A.V. Khvalkovskiy, J. Grollier, A. Dussaux, K.A. Zvezdin, V. Cros. Phys. Rev. B **80**, 14040 (2009).
[15] Y. Gaididei, V. Kravchuk, D. Sheka. J. Int. Quantum Chem. **110**, 8397 (2010).
[16] B.A. Ivanov, E. Zaspel. Phys. Rev. Lett. **99**, 247208 (2007).
[17] N.A. Usov, S.E. Peschanyi. Fiz. Met. Metalloved. **78**, *6*, 13 (1994). (in Russian).

[18] K.Y. Guslienko, K.S. Buchanan, S.D. Bader, V. Novosad. Appl. Phys. Lett. **86**, 223112 (2005).
[19] N. Locatelli, V.V. Naletov, J. Grollier, G. de Loubens, V. Cros, C. Deranlot, C. Ulysse, G. Faini, O. Klein, A. Fert. Appl. Phys. Lett. **98**, *6*, 062501 (2011).
[20] S.S. Cherepov, B.C. Koop, A.Y. Galkin, R.S. Khymyn, B.A. Ivanov, D.C. Worledge, V. Korenivski. Phys. Rev. Lett. **109**, 097204 (2012).
[21] N. Locatelli, A.E. Ekomasov, A.V. Khvalkovskiy, S.A. Azamatov, K.A. Zvezdin, J. Grollier, E.G. Ekomasov, V. Cros. Appl. Phys. Lett. **102**, 062401 (2013).
[22] V. Sluka, A. Kakay, A.M. Deac, D.E. Burgler, C.M. Schneider, R. Hertel. Nature Commun. **6**, 6409 (2015).
[23] N. Locatelli, R. Lebrun, V. Naletov, A. Hamadeh, G. De Loubens, O. Klein, J. Grollier, V. Cros. IEEE Trans. Magn. **51**, 4300206 (2015).
[24] E. Holmgren, A. Bondarenko, B.A. Ivanov, V. Korenivski. Phys. Rev. **97**, 094406 (2018).
[25] Anam Hanif, Arbab Abdur Rahim, Husnul Maab. Condens. Matter **668**, 415203 (2023).
[26] A. Ekomasov, S. Stepanov, K. Zvezdin, E. Ekomasov. Phys. Met. Met. **118**, *4*, 328 (2017).
[27] S. Stepanov, A. Ekomasov, K. Zvezdin, E. Ekomasov. Phys. Solid State **60**, *6*, 1055 (2018).
[28] A.E. Ekomasov, S.V. Stepanov, K.A. Zvezdin, E.G. Ekomasov. J. Magn. Magn. Mater. **471**, 513 (2019).
[29] E.G. Ekomasov, S.V. Stepanov, V.N. Nazarov, K.A. Zvezdin, N.G. Pugach, G.I. Antonov. Tech. Phys. Lett. **47**, *9*, 870 (2021).
[30] S.V. Stepanov, V.N. Nazarov, K.A. Zvezdin, E.G. Ekomasov. JMMM **562**, 169758 (2022).
[31] A.V. Khvalkovskiy, J. Grollier, N. Locatelli, Y.V. Gorbunov, K.A. Zvezdin, V. Cros. Appl. Phys. Lett. **96**, 212507 (2010).
[32] A.V. Khvalkovskiy, J. Grollier, A. Dussaux, K.A. Zvezdin, V. Cros. Phys. Rev. B **80**, 140401 (2009).

Translated by D.Safin